



Since January 2020 Elsevier has created a COVID-19 resource centre with free information in English and Mandarin on the novel coronavirus COVID-19. The COVID-19 resource centre is hosted on Elsevier Connect, the company's public news and information website.

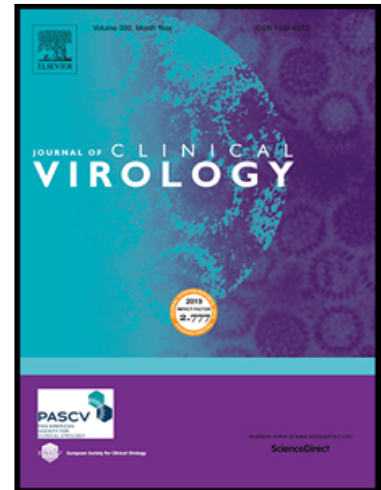
Elsevier hereby grants permission to make all its COVID-19-related research that is available on the COVID-19 resource centre - including this research content - immediately available in PubMed Central and other publicly funded repositories, such as the WHO COVID database with rights for unrestricted research re-use and analyses in any form or by any means with acknowledgement of the original source. These permissions are granted for free by Elsevier for as long as the COVID-19 resource centre remains active.

## Journal Pre-proof

Sierra SARS-CoV-2 Sequence and Antiviral Resistance Analysis Program

Philip L. Tzou , Kaiming Tao , Malaya K. Sahoo ,  
Sergei L. Kosakovsky Pond , Benjamin A. Pinsky ,  
Robert W. Shafer

PII: S1386-6532(22)00255-4  
DOI: <https://doi.org/10.1016/j.jcv.2022.105323>  
Reference: JCV 105323



To appear in: *Journal of Clinical Virology*

Received date: 26 June 2022  
Revised date: 11 October 2022  
Accepted date: 21 October 2022

Please cite this article as: Philip L. Tzou , Kaiming Tao , Malaya K. Sahoo , Sergei L. Kosakovsky Pond , Benjamin A. Pinsky , Robert W. Shafer , Sierra SARS-CoV-2 Sequence and Antiviral Resistance Analysis Program, *Journal of Clinical Virology* (2022), doi: <https://doi.org/10.1016/j.jcv.2022.105323>

This is a PDF file of an article that has undergone enhancements after acceptance, such as the addition of a cover page and metadata, and formatting for readability, but it is not yet the definitive version of record. This version will undergo additional copyediting, typesetting and review before it is published in its final form, but we are providing this version to give early visibility of the article. Please note that, during the production process, errors may be discovered which could affect the content, and all legal disclaimers that apply to the journal pertain.

© 2022 The Author(s). Published by Elsevier B.V.

This is an open access article under the CC BY license (<http://creativecommons.org/licenses/by/4.0/>)

**TITLE**

Sierra SARS-CoV-2 Sequence and Antiviral Resistance Analysis Program

**AUTHORS**

Philip L. Tzou<sup>1</sup>, Kaiming Tao<sup>1</sup>, Malaya K. Sahoo<sup>2</sup>, Sergei L. Kosakovsky Pond<sup>3</sup>, Benjamin A. Pinsky<sup>2</sup>, Robert W. Shafer<sup>1</sup>

**AFFILIATIONS**

<sup>1</sup>Division of Infectious Diseases, Department of Medicine, Stanford University, Stanford, CA, USA;

<sup>2</sup>Department of Pathology, Stanford University, Stanford, CA, USA; <sup>3</sup>Institute for Genomics and Evolutionary Medicine, Temple University, Philadelphia, Pennsylvania, USA.

**CORRESPONDING AUTHOR:** Philip L. Tzou (philiptz@stanford.edu) and Robert W. Shafer (rshefer@stanford.edu)

**WORD COUNT:** 2,498

- Sierra SARS-CoV-2 provides quality control and annotation for viral genomic data.
- Sierra SARS-CoV-2 is highly concordant with established sequence analysis programs.
- 300 SARS-CoV-2 Spike mutations reduce susceptibility to monoclonal antibodies.
- Approximately 20 RdRP and Mpro mutations reduce antiviral susceptibility in vitro.
- Sierra SARS-CoV-2 has susceptibility data for 88% of Spike RBD mutation patterns.

**ABSTRACT**

Introduction: Although most laboratories are capable of employing established protocols to perform full-genome SARS-CoV-2 sequencing, many are unable to assess sequence quality, select appropriate mutation-detection thresholds, or report on the potential clinical significance of mutations in the targets of antiviral therapy. Methods: We describe the technical aspects and benchmark the performance of

30 Sierra SARS-CoV-2, a program designed to perform these functions on user-submitted FASTQ and FASTA  
31 sequence files and lists of Spike mutations. Sierra SARS-CoV-2 indicates which sequences contain an  
32 unexpectedly large number of unusual mutations and which mutations are associated with reduced  
33 susceptibility to clinical stage mAbs, the RdRP inhibitor remdesivir, or the Mpro inhibitor nirmatrelvir.  
34 Results: To assess the performance of Sierra SARS-CoV-2 on FASTQ files, we applied it to 600  
35 representative FASTQ sequences and compared the results to the COVID-19 EDGE program. To assess its  
36 performance on FASTA files, we applied it to nearly one million representative FASTA sequences and  
37 compared the results to the GISAID mutation annotation. To assess its performance on mutations lists,  
38 we applied it to 13,578 distinct Spike RBD mutation patterns and showed that exactly or partially  
39 matching annotations were available for 88% of patterns. Conclusion: Sierra SARS-CoV-2 leverages  
40 previously published data to improve the quality control of submitted viral genomic data and to provide  
41 functional annotation on the impact of mutations in the targets of antiviral SARS-CoV-2 therapy. The  
42 program can be found at <https://covdb.stanford.edu/sierra/sars2/> and its source code at  
43 <https://github.com/hivdb/sierra-sars2>.

44

45 Keywords: SARS-CoV-2; genomic sequencing; mutations; antiviral resistance

46

## INTRODUCTION

47

48

SARS-CoV-2 sequencing is performed for surveillance as well as research and clinical purposes.

49

The extent of sequencing for clinical purposes may increase as more SARS-CoV-2 inhibitors become

50

available, particularly if resistance to these inhibitors arises. Although most laboratories are capable of

51

performing full-genome SARS-CoV-2 sequencing employing established laboratory and sequence

52

analysis protocols [1–8], many are unable to assess sequence quality, select appropriate mutation-

53

detection thresholds, or report the potential clinical significance of SARS-CoV-2 mutations in the targets

54

of antiviral therapy.

55

We previously briefly described a sequence analysis program called Sierra SARS-CoV-2 in a paper

56

on the Stanford Coronavirus Antiviral Resistance Database (CoV-RDB) [9]. The program utilizes the same

57

codebase as Sierra HIV [10,11], the Stanford HIV Drug Resistance Database sequence analysis program

58

[10,11]. The program accepts three types of input: FASTQ files containing short reads from a deep

59

sequencing instrument, FASTA sequences, and lists of Spike amino acid mutations.

60

To assess the performance of Sierra SARS-CoV-2 on FASTQ files, we applied it to two sets of

61

sequences from the NCBI Sequence Read Archive (SRA) [12] and to sequences from a clinical laboratory.

62

To assess its performance on consensus FASTA sequences, we applied it to 963,237 SARS-CoV-2 genome

63

sequences from GISAID [13]. To assess its performance interpreting Spike mutations, we applied it to

64

13,578 distinct Spike receptor binding domain (RBD) amino acid mutation patterns from approximately

65

4.7 million SARS-CoV-2 GISAID sequences.

66

67

## METHODS

68

Sierra SARS2-CoV-2 provides native support for FASTA sequences and lists of mutations, defined

69

as amino acid differences from the Wuhan-Hu-1 reference sequence (GenBank accession NC\_045512.2).

70

Support for FASTQ files is provided through an auxiliary pipeline that converts FASTQ files to comma-

71 delimited files containing the frequency of each codon at each genomic position, i.e., codon frequency  
72 (CodFreq) files [9,11]. Table 1 summarizes SARS-CoV-2 output depending on whether CodFreq files,  
73 FASTA sequences, or mutation lists are submitted. Figure 1 illustrates the workflow of Sierra SARS2-CoV-  
74 2 for all three input types.

75

#### 76 **Generation of CodFreq files and consensus sequences**

77 CodFreq files contain seven columns: gene, amino acid position, number of reads at a position,  
78 codon, number of reads for a codon, amino acid, and proportion of reads for a codon. For our  
79 application, the CodFreq format has several advantages over the commonly used variant call format  
80 (VCF) because CodFreq files can be interpreted without a reference sequence and used independently  
81 from the accompanying SAM/BAM file. CodFreq files can be used to generate a consensus FASTA  
82 sequence containing mixtures of codons above a user-specified threshold.

83 The CodFreq pipeline can be run on batched sequences using the Sierra SARS2-CoV-2 frontend  
84 or locally using a pre-built Docker image. A shell script is provided on GitHub for running the CodFreq  
85 pipeline from a local host (<https://github.com/hivdb/codfreq>). The frontend identifies paired-end files  
86 and prompts users to confirm the pairing. An advanced option is provided for users submitting primer  
87 information. The pipeline reports progress for each backend task.

88 The CodFreq pipeline includes the following steps (Supplementary Figure): (1) The Fastp  
89 program trims adapters, removes regions with low phred scores, and stitches paired reads; (2)  
90 MiniMap2 aligns FASTQ sequence reads to the reference sequence [14]; (3) Samtools converts the  
91 resulting SAM text file into a binary BAM file and a BAI index file [15]; (4) PySam reads the BAM file to  
92 determine the frequency of each codon at each position; and (5) PostAlign, a program we created,  
93 adjusts the placement of indels through a codon-aware process (<https://github.com/hivdb/post-align>).

94 Depending on user input, the programs Cutadapt or iVar are used to trim SARS-CoV-2 primers [16,17].

95 The CodFreq and BAM files are provided for users to download.

96

### 97 **Identification of amino acid mutations and lineage assignment**

98 Minimap2 and PostAlign are used to analyze FASTA sequences. Minimap2 aligns a query  
99 sequence to the reference sequence and saves the alignment in Pairwise mApping Format (PAF) files,  
100 which are then loaded into pairwise nucleotide alignments. PostAlign adjusts indels using a codon aware  
101 process and position-specific gap scores to increase consistency of indel placement in accordance with  
102 alignments of established SARS-CoV-2 variants. PostAlign also separates alignments into discrete genes,  
103 identifies mutations, and numbers them by gene. If complete genomes are submitted, the Pangolin  
104 program is used to assign the PANGO lineage [18].

105

### 106 **Report generation and mutation annotation**

107 The Sierra SARS-CoV-2 report contains sections summarizing sequence and mutation data  
108 (Supplementary File). The sequence summary reports the genes present in a sequence, areas in which  
109 sequence data are missing, the consensus sequence, and the assigned PANGO lineage. It contains a  
110 figure plotting read coverage along the sequence and read depths for Mpro, RdRp, and Spike genes.  
111 Dropdown menus enable users to interactively adjust the minimum number and proportion of reads for  
112 reporting non-consensus mutations.

113 Each mutation in a sequence is annotated with the following information: (1) The proportion  
114 and number of reads containing the mutation; (2) Whether the mutation is unusual, defined as having a  
115 global prevalence below 0.01% based on the open-source sequence analysis pipeline created by the  
116 Kosakovsky Pond laboratory [19]; (3) Whether the mutation is an mAb resistance mutation defined as a  
117 Spike mutation associated with reduced susceptibility to one or more clinical-stage mAbs; (4) Whether

118 the mutation is a potential RdRp or Mpro resistance mutation; and (5) Comments for the most well  
119 studied Spike mutations associated with reduced mAb susceptibility and for most mutations associated  
120 with Mpro and RdRp inhibitor reduced susceptibility. The lists of mAb and potential RdRp and Mpro  
121 resistance mutations are updated monthly.

122 Each list of Spike mutations is also used to interrogate CoV-RDB for published mAb,  
123 convalescent plasma, and vaccinee plasma susceptibility data. There is an option to display just data  
124 from variants with exactly matching sets of mutations versus comprehensive results with data for  
125 variants with a subset or superset of the submitted mutations.

126

#### 127 **Generating a list of mAb resistance mutations**

128 mAb resistance mutations were defined as Spike mutations with a median  $\geq 5$  fold reduction in  
129 susceptibility compared with wildtype according to CoV-RDB and/or having an escape fraction  $\geq 0.1$  in  
130 the deep mutational scanning (DMS) platform developed by the Bloom Laboratory at the University of  
131 Washington [20,21]. As of September 2022, there were 488 spike mutations meeting these criteria.  
132 Figure 2 illustrates the 160 RBD-associated mAb-resistance mutations having a prevalence  $\geq 0.0001\%$   
133 with data on their neutralizing antibody susceptibilities, DMS escape fractions, and whether they were  
134 selected *in vitro* and/or *in vivo*.

135

#### 136 **Generating a list of mutations associated with potential small molecule inhibitor resistance**

137 Mpro and RdRp mutations were classified as potential drug-resistance mutations if they met  
138 one of the following three criteria: (1) they were associated with 2.5-fold or higher reductions in  
139 susceptibility in either a biochemical assay or in cell culture; (2) they were selected during an *in vitro*  
140 passage experiment; or (3) they were selected in a person receiving an Mpro or RdRp inhibitor. Figure 3  
141 illustrates that as of September 2022, 42 mutations at 28 positions were reported to be possibly



142 associated with reduced susceptibility to Mpro inhibitors nirmatrelvir or ensitrelvir [22–35], and 11  
143 mutations at 9 positions were reported to be possibly associated with reduced susceptibility to the RdRp  
144 inhibitor remdesivir [36–43].

145

#### 146 **Datasets used for benchmarking and validation**

147 FASTQ files: Three sets of NGS files were used to compare the results of the CodFreq pipeline  
148 with the LANL EDGE COVID-19 program [3] including 200 randomly selected Illumina files obtained  
149 between March 2021 and March 2022 from the NCBI SARS-CoV-2 SRA portal, 200 randomly selected  
150 Oxford Nanopore Technology (ONT) files obtained March 2022 from the SRA portal, and 200 Illumina  
151 sequences from the Stanford University Hospital (SUH) Diagnostic Virology Laboratory between April  
152 2021 and March 2022. Pangolin 4.0.5 classified 52.8% of the 600 sequences as Delta variants, 27.8% as  
153 Omicron variants, 11.6% as Alpha variants, and 7.8% as other variants. For the SRA sequences, we used  
154 the parameter `–skip-technical` to exclude adapters, primers, and bar-codes from the downloaded FASTQ  
155 file. The SUH sequences were generated using a recently published pipeline [44].

156 FASTA files: On March 25, 2022, a random set of 963,237 FASTA files was selected from  
157 9,632,370 GISAID sequences[45].

158 Mutation data: The global prevalence of each Spike, Mpro and RdRp mutation was obtained  
159 from a publicly available quality controlled analysis pipeline created by the Kosakovsky Pond laboratory  
160 that contained 4,740,761 Spike, 5,328,735 Mpro, and 5,076,452 RdRp sequences containing 201,167  
161 Spike, 5,404, Mpro and 32,788 RdRp distinct mutation patterns [46,47].

162

## 163 **RESULTS**

### 164 **FASTQ files**

165 To evaluate the CodFreq pipeline using FASTQ files, we tested the 200 NCBI SRA Illumina files,  
166 the 200 NCBI SRA ONT files and the 200 SUH Illumina files. For the 400 Illumina and 200 ONT sequences,  
167 we compared the consensus codon of each CodFreq file to the codon in the consensus FASTA file  
168 generated by the EDGE COVID-19 program (version 20220314). For both pipelines, a codon-level read  
169 depth  $\geq 5$  and a mutation-detection threshold of 50% were used.

170 Illumina sequences: For regions successfully aligned by both Sierra and EDGE, each program  
171 detected a mean 11.0, 1.7, and 0.19 amino acid mutations per sequence in Spike, RdRp, and Mpro. Of  
172 the 4,413 Spike mutations detected by either program, Sierra and EDGE detected the same mutation in  
173 98.9% of cases; 0.7% were detected only by Sierra and 0.3% only by EDGE. Of 760 RdRp and Mpro  
174 mutations, Sierra and EDGE detected the same mutation in 98.4% of cases; 1.5% were detected only by  
175 Sierra and 0.1% only by EDGE. The 59 discordances in the three genes resulted from small differences in  
176 the threshold at which mutations were detected ( $n=49$ ) and in placement of indels ( $n=10$ ).

177 ONT sequences: For regions successfully aligned by both Sierra and EDGE, Sierra detected a  
178 mean 19.0, 1.7, and 0.48 mutations and EDGE detected a mean 18.7, 1.7, and 0.49 mutations per  
179 sequence in Spike, RdRp, and Mpro. Of the 3,855 Spike mutations detected by either program, Sierra  
180 and EDGE detected the same mutation in 94.3% of cases; 3.8% were detected only by Sierra and 2.0%  
181 only by EDGE. Of 448 detected RdRp and Mpro mutations, Sierra and EDGE detected the same mutation  
182 in 96.9% of cases; 2.0% were detected only by Sierra and 1.1% only by EDGE. The 235 discordances in  
183 the three genes resulted from small differences in the threshold at which mutations were detected  
184 ( $n=174$ ) and in the placement of indels ( $n=61$ ).

185

#### 186 **FASTA files**

187 We compared the Spike, Mpro, and RdRp mutation lists generated by Minimap2 and PostAlign  
188 with the GISAID "AA substitutions" metadata, generated by the CoVServer program [45] for 963,237

189 FASTA sequences. The list of mutations for Spike, Mpro, and RdRp genes identified by Sierra and GISAID  
190 were identical for 99.4%, 99.9% and 99.5% of sequences, respectively. However, there were differences  
191 in the placement of indels for Spike. Nearly all Spike differences were caused by indels at several  
192 positions, such as the Omicron BA.1 N-terminal domain deletion that has alternatively been placed at  
193 position 211 [48,49] or 212 [50–52]. The non-indel differences resulted from how mutations in regions  
194 surrounding missing sequence data were handled.

195

#### 196 **Mutation lists**

197 Distribution of usual and unusual mutations: Figures 4A-C show the number of mutations in  
198 Spike, RdRP, and Mpro genes by the binned global prevalence of each mutation. Spike had 694 usual  
199 and 8,501 unusual non-indel mutations. RdRp had 300 usual and 4,192 unusual non-indel mutations.  
200 Mpro had 107 usual and 1,579 unusual non-indel mutations.

201 Figures 5A-C show the number of unusual mutations per sequence in Spike, RdRP, and Mpro. In  
202 Spike, 92.9% sequences had no unusual mutations, 6.7% had one, 0.4% had two, and <0.1% had three or  
203 more unusual mutations. In RdRp, 96.1% sequences had no unusual mutation, 3.8% had one and 0.1%  
204 had two or more unusual mutations. In Mpro, 99.2% sequences had no unusual mutation, 0.7% had one  
205 and 0.1% had two or more unusual mutations.

206 Figure 6 shows the numbers of usual and unusual Spike mutations at different mutation  
207 thresholds in the 200 NCBI Illumina and 200 NCBI ONT sequences. At mutation detection thresholds  
208 <50%, there was a markedly higher proportion of unusual mutations in ONT compared with Illumina  
209 sequences.

210 Neutralizing susceptibility data in CoV-RDB for submitted RBD mutation patterns: The Spike  
211 mutation pattern dataset contained 13,578 distinct patterns of Spike RBD mutations. Each RBD mutation  
212 pattern was submitted to Sierra to determine the frequency for which complete or partial neutralizing

213 susceptibility data was available in CoV-RDB [9](Figure 7). For 76.7% of sequences (1.3% of patterns),  
214 CoV-RDB contained data exactly matching the submitted mutation pattern. For 10.2% of sequences  
215 (86.6% of patterns), CoV-RDB contained data partially matching the submitted mutation pattern (i.e.,  
216 CoV-RDB contained data for mutation patterns representing a subset, superset, or intersecting set of the  
217 mutations in the submitted mutation pattern). For 13.0% of sequences (12.0% of patterns), CoV-RDB  
218 contained no data matching the pattern of submitted mutations.

219

220

## DISCUSSION

221 Sierra SARS-CoV-2 is an open-source web-based program that accepts FASTQ and FASTA files  
222 and lists of Spike mutations. Depending on the nature of the input data, it generates a consensus  
223 nucleotide sequence, assigns a sequence lineage, identifies amino acid mutations, and uses the  
224 mutations to interrogate a quality-controlled sequence analysis pipeline for global mutation prevalence  
225 data and CoV-RDB for data on SARS-CoV-2 susceptibility to antiviral agents and to plasma from  
226 previously infected and/or vaccinated persons.

227 We assessed the performance of Sierra SARS-CoV-2 using 600 FASTQ datasets, nearly one  
228 million FASTA sequences, and approximately 13,500 distinct Spike RBD mutation patterns. In the  
229 analysis of FASTQ sequences, Sierra SARS-CoV-2 and EDGE COVID-19 were highly concordant and in the  
230 analysis of FASTA sequences, Sierra SARS-CoV-2 and the GISAID mutation list were highly concordant.  
231 For both analyses, most discordances resulted from equally acceptable placements of several commonly  
232 occurring indels. An analysis of approximately 13,500 distinct Spike RBD mutation patterns, showed that  
233 exactly or partially matching annotation data were available for 88% of reported mutation patterns.

234 Sierra SARS-CoV-2 uses mutation prevalence data to identify sequences with an unexpectedly  
235 large number of unusual mutations. Indeed, only 0.1% of quality-controlled Spike sequences had three  
236 or more unusual mutations and only 0.1% of quality-controlled Mpro and RdRp sequences had two or

237 more unusual mutations. Therefore, the presence of many unusual mutations in a sequence suggests  
238 the possibility of sequence artifact or possibly, although less likely, a novel variant.

239 Sierra SARS-CoV-2 uses published data to identify mutations potentially associated with reduced  
240 antiviral susceptibility. Although few major SARS-CoV-2 lineages circulate at any time, an increasing  
241 number of Omicron sub-variants containing different spike mutation patterns are now reported in many  
242 regions [53]. Therefore, a sequence analysis program that provides susceptibility data for mutation  
243 patterns, as well as for variants of concern has become increasingly relevant. Additionally, an increasing  
244 number of Mpro mutations associated with reduced nirmatrelvir susceptibility have been identified *in*  
245 *vitro*, although few have been reported in persons receiving nirmatrelvir.

246 In conclusion, Sierra SARS-CoV-2 is one of a few open-source analytic pipelines actively  
247 maintained and available through a web interface [3,6,7]. It uniquely leverages published data to  
248 improve the quality control of submitted viral genomic data and to provide functional annotation on the  
249 impact of mutations in the targets of antiviral therapy.

250

#### 251 **ACKNOWLEDGMENTS**

252 PLT, KT, and RWS have been funded in part by a grant from the NIH/NIAID: AI136618. The funder played  
253 no role in this study.

254 RWS served on Gilead Sciences and Vir Biotechnologies/GlaxoSmithKline scientific advisory boards.

255

256

257

258

## FIGURE LEGENDS

259 Figure 1

260 Sierra SARS-CoV-2 work flow for handling FASTQ files, FASTA files, and lists of SARS-CoV-2 mutations.

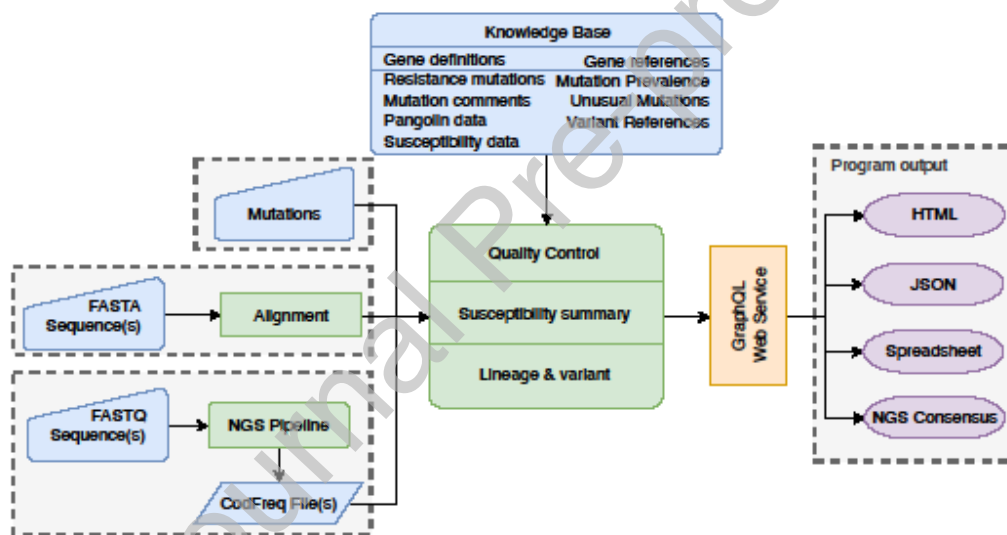
261 Sierra provides native support for FASTA sequences and mutation lists. Support for FASTQ files is

262 provided through an auxiliary pipeline that converts FASTQ files into CSV files containing the frequency

263 of each codon at each position in a genome. The workflow for the auxiliary pipeline is shown in

264 Supplementary Figure. The Supplementary File shows an example of the HTML output.

265



266

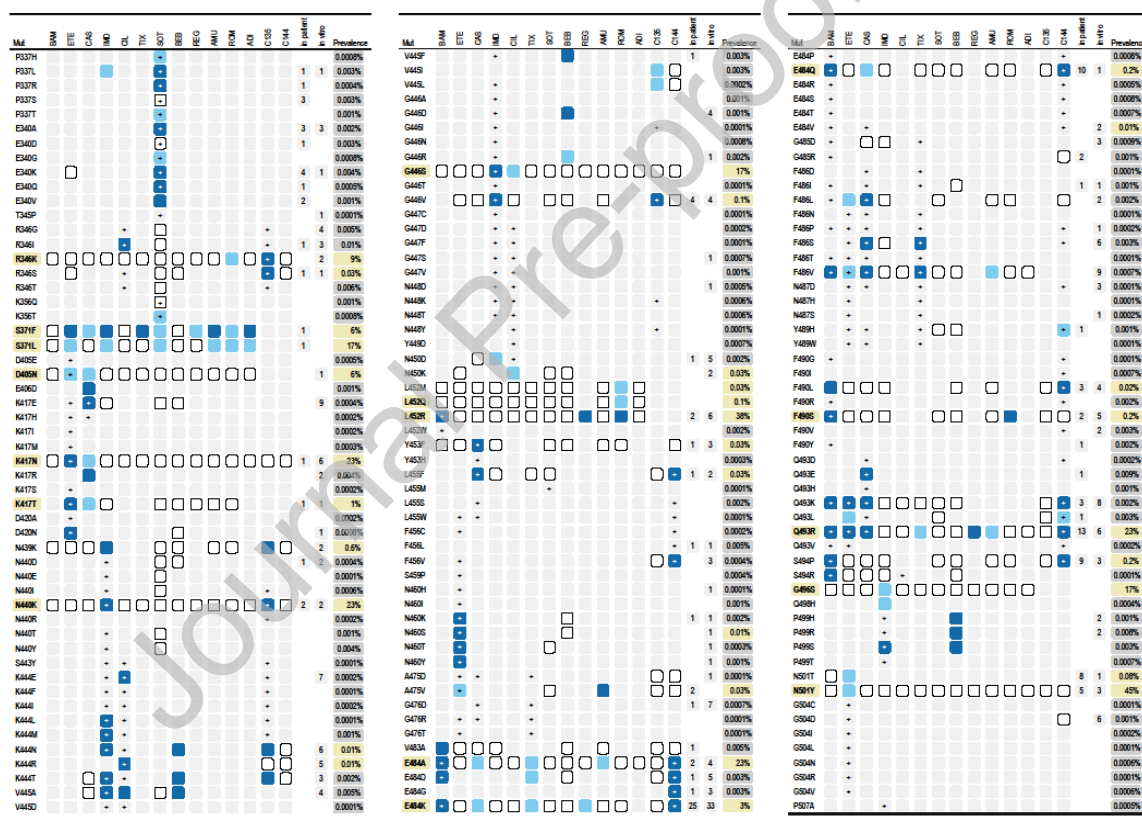
267

268 Figure 2

269 SARS-CoV-2 Spike RBD mAb-resistance mutations. The mAb-resistance mutations shown met one or

270 more of the following criteria: (1) having a  $\geq 5$ -fold reduction in susceptibility to a clinical stage mAb; (2)271 having a DMS escape fraction  $\geq 0.1$  and having a global prevalence  $> 0.001\%$ ; (3) having been selected *in*272 *vitro* by an mAb; or (4) having been selected *in vivo* in a patient receiving an mAb or experiencing

273 prolonged infection. A dark blue cell indicates a  $\geq 25$ -fold reduction in susceptibility; a light blue cell  
 274 indicates a 5-25-fold reduction in susceptibility; a white cell indicates a  $< 5$ -fold reduction in susceptibility;  
 275 and a gray cell indicates the absence of susceptibility data. Cells with a plus (+) symbol indicates that the  
 276 mutation had a DMS escape fraction  $\geq 0.1$ . Bold mutations with a yellow background represent the  
 277 consensus for one or more variants of concern or of interest. The numbers in the “in vivo” column  
 278 indicate the numbers of times the mutation was selected *in vivo* during prolonged infection or in a  
 279 patient receiving an mAb. The numbers in the “in vitro” column indicate the number of times the  
 280 mutation was reported to be selected during passage in the presence of an mAb.



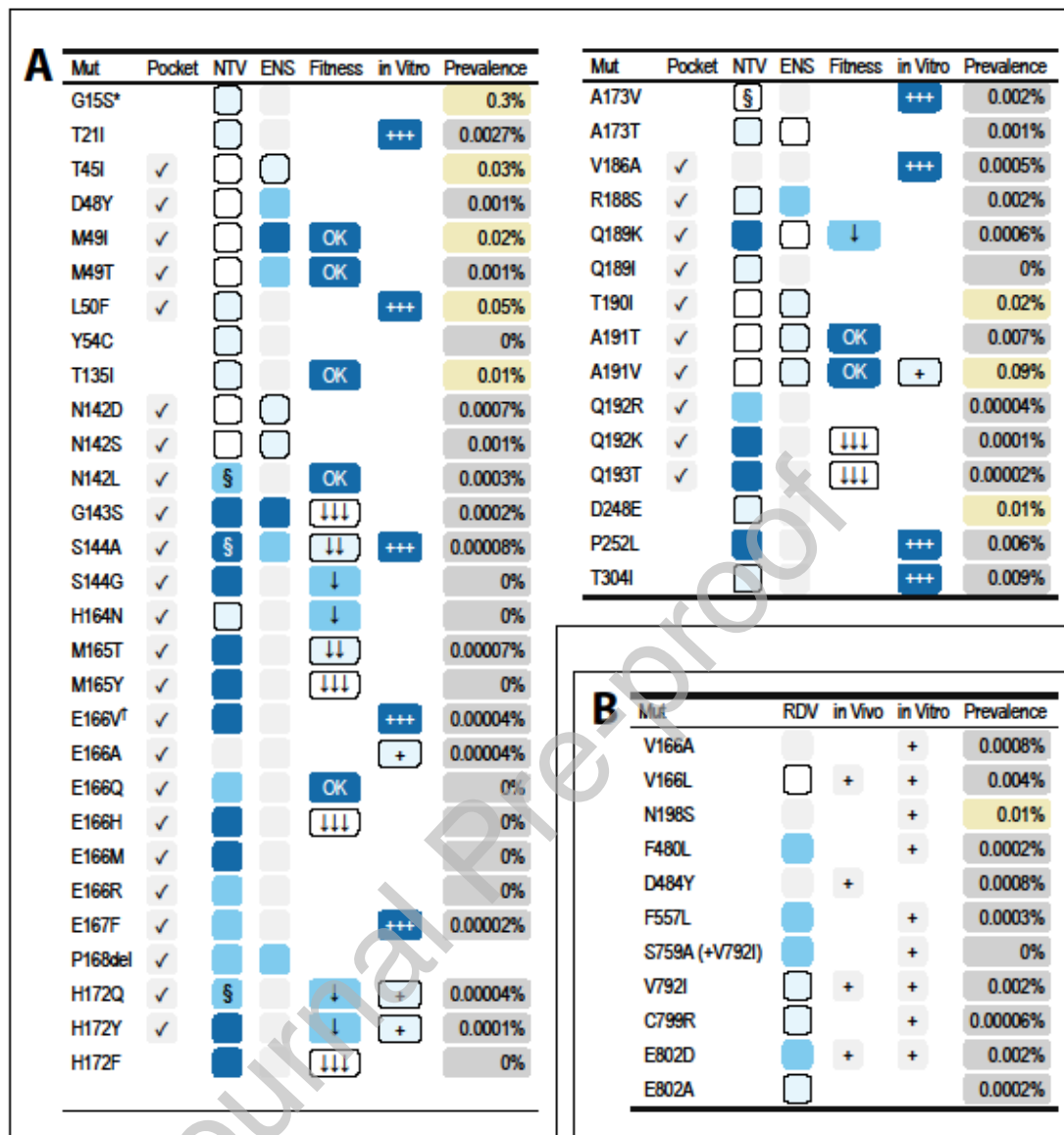
281

282 Figure 3

283 SARS-CoV-2 Mpro (A) and RdRp (B) resistance mutations. For Mpro, the figure shows which mutations  
 284 are in the Mpro substrate binding pocket [34,35], which are associated with reduced susceptibility to  
 285 nirmatrelvir (NTV) or ensitrelvir (ENS) either biochemically or in cell culture, which have been selected *in*

286 *vitro*, the effect of mutations on Mpro fitness determined either biochemically or in cell culture, and the  
287 global mutation prevalence as of June 2022. For RdRp, the figure shows which mutations reduced  
288 susceptibility to remdesivir (RDV), which have been selected by RDV *in vitro* and *in vivo*, and the global  
289 mutation prevalence as of June 2022. A dark blue cell indicates  $\geq 10$ -fold reduction in susceptibility; a  
290 light blue cell indicates 5-10-fold reduction; a very light blue cell indicates a 2.5-5-fold reduction; and a  
291 white cell indicates a  $< 2.5$ -fold reduction. A gray cell indicates the absence of susceptibility data. \*G15S  
292 is the consensus amino acid for the Lambda variant. †E166V has been reported in three persons  
293 receiving nirmatrelvir in the EPIC-HR study [22]. §Variable reductions in susceptibility were reported for  
294 this mutation in different studies. For RDV, S759A was evaluated only in combination with V792I; F480L  
295 and F557L were evaluated only in combination with each other.  
296



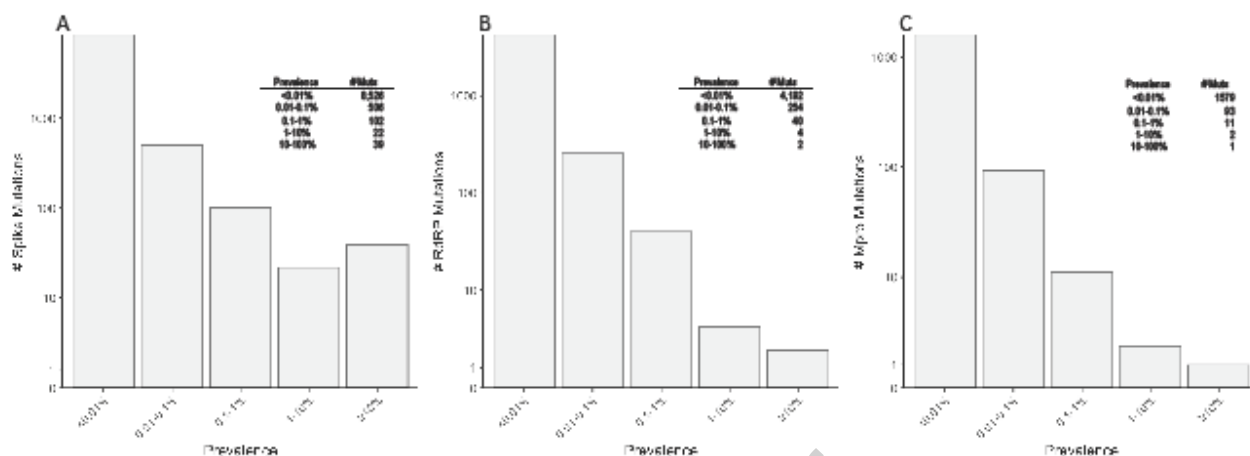


297

298 Figure 4

299 The numbers of Spike, RdRP, and Mpro mutations according to their global prevalence (A-C). The  
 300 histograms represent the numbers of mutations on a log<sub>10</sub> scale within five prevalence ranges (≥10%,  
 301 1%-10%, 0.1%-1%, 0.01%-0.1%, and <0.01%) in 4,740,761 quality-controlled sequences. Mutations that  
 302 were never reported were not counted. The insets in each plot contain the actual numbers represented  
 303 by the histograms.

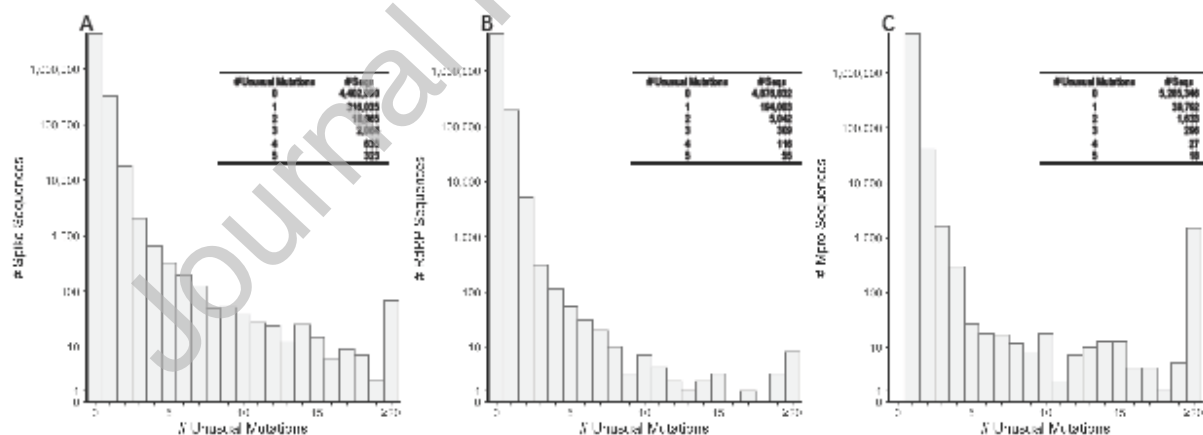
304



305

306 Figure 5

307 The distribution in the numbers of unusual mutations per sequence in Spike, RdRp, and Mpro in  
 308 4,740,761 quality-controlled sequences (A-C). The histograms represent the numbers of sequences on a  
 309  $\log_{10}$  scale according to the number of unusual mutations per sequence. The insets in each plot contain  
 310 the numbers represented by the first six histograms.



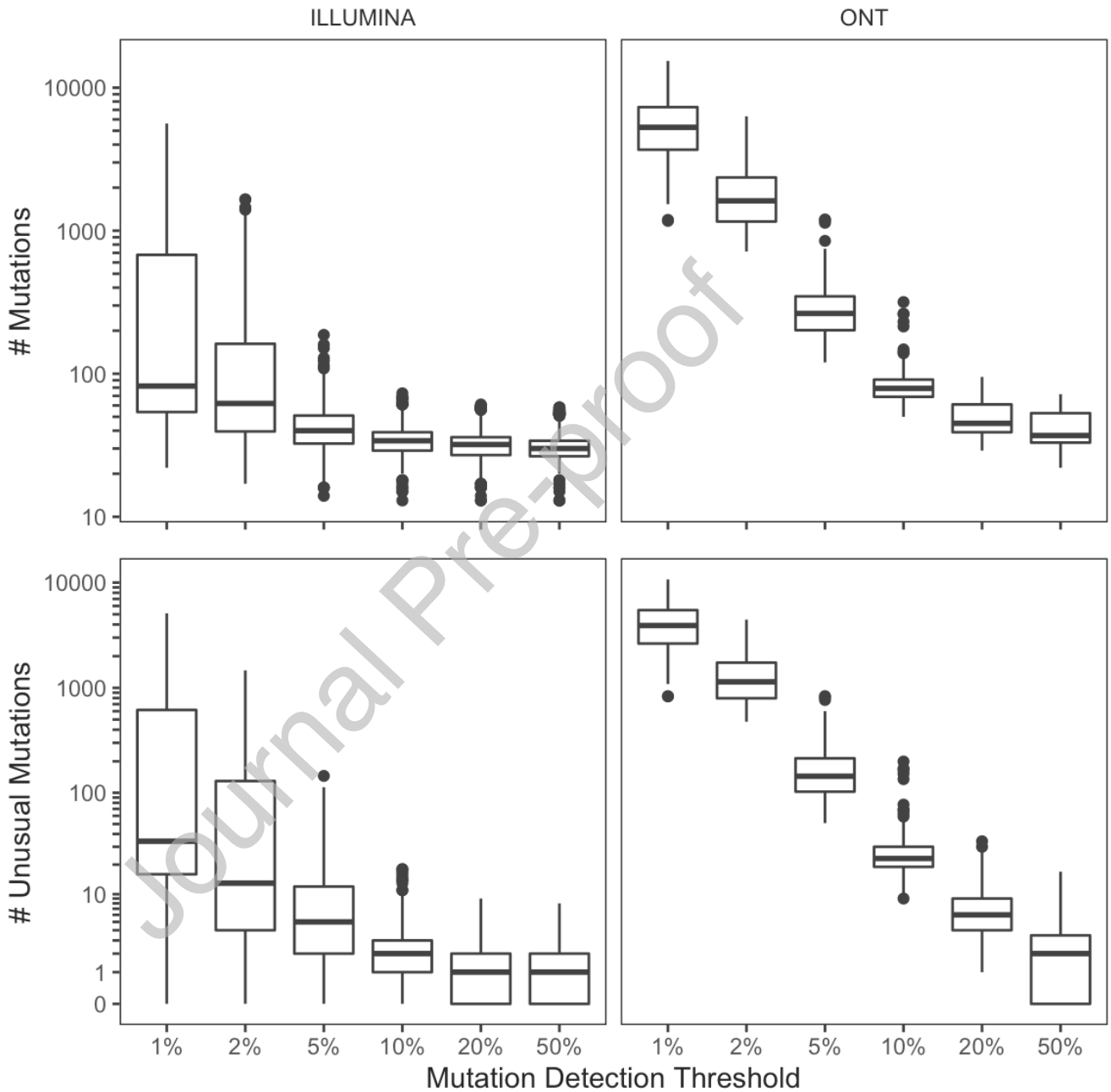
311

312

313 Figure 6

314 Box plots indicating the numbers of usual and unusual mutations per genome at different mutation  
 315 thresholds for the 400 Illumina and 200 ONT sequences in the FASTQ dataset. The boxplots show the

316 median and inter-quartile ranges (IQRs). The whiskers extend  $\pm 1.5$  IQRs from the hinge. Regions for  
317 which the median read depth was  $<100$  were excluded.

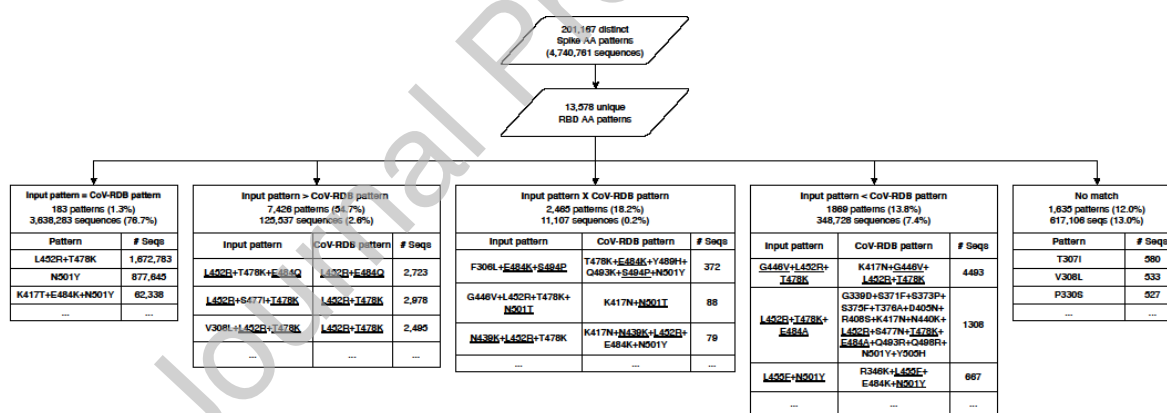


318

319

320 Figure 7

321 Availability of neutralizing susceptibility data in CoV-RDB for submitted sets of Spike receptor binding  
 322 domain (RBD) mutations. The 13,578 unique patterns of RBD mutations, present in 4,740,761 sequences,  
 323 were submitted to Sierra SARS-CoV-2. Exactly matching susceptibility data were available for 183  
 324 mutation patterns (1.3% of mutation patterns derived from 76.7% of sequences). Partially matching  
 325 susceptibility data were available for 11,760 patterns (86.6% of patterns from 10.2% of sequences)  
 326 including cases for which CoV-RDB contained data for a subset, superset, or intersecting set of mutation  
 327 patterns. No matching susceptibility data were available for 1,635 mutation patterns (12.0% of patterns  
 328 from 13.0% of sequences). Each of the five tables contain examples of the five scenarios: exact match,  
 329 subset, superset, intersection, and no match with one column showing the submitted mutation pattern,  
 330 another showing the closest CoV-RDB pattern, and the third showing the number of sequences (except  
 331 for the tables showing the patterns that contained an exact match or no match in CoV-RDB).



333

334

335

336

337 Table 1. Overview of the Sierra SARS2-CoV-2 Analysis Report

Feature	Input Type <sup>1</sup>		
	FASTQ	FASTA	Mutations
<b>Sequence summary</b>			
Gene list	✓	✓	
PANGO lineage <sup>2</sup>	✓	✓	
Median read depth	✓		
Interactive mutation detection thresholds	✓		
Consensus sequence with IUPAC nucleotides <sup>3</sup>	✓		
<b>Sequence quality assessment</b>			
List of unsequenced regions	✓	✓	
List of unusual mutations	✓	✓	
List of low-coverage regions	✓		
<b>Mutation summaries</b>			
Prevalence of each mutation in a sample	✓		
mAb susceptibility summaries	✓	✓	✓
Mutation-specific annotation	✓	✓	✓
Convalescent and vaccinee plasma susceptibility data	✓	✓	✓

338

339 Footnote: <sup>1</sup>FASTQ indicates the raw data associated with an NGS platform, most commonly Illumina and

340 Oxford Nanopore Technologies; FASTA sequences are usually derived from the consensus of NGS data.

341 Mutations indicate user submitted amino acid differences from the consensus Wuhan-Hu-1 Spike

342 sequence. <sup>2</sup>PANGO – Phylogenetic Assignment of Named Global Outbreak. <sup>3</sup>IUPAC – International Union

343 of Pure and Applied Chemistry representation of nucleotide ambiguities or mixtures

344

345

346

## REFERENCES

- 347 [1] C. Charre, C. Ginevra, M. Sabatier, H. Regue, G. Destras, S. Brun, G. Burfin, C. Scholtes,  
348 F. Morfin, M. Valette, B. Lina, A. Bal, L. Josset, Evaluation of NGS-based approaches for  
349 SARS-CoV-2 whole genome characterisation, *Virus Evol.* 6 (2020) veaa075.  
350 <https://doi.org/10.1093/ve/veaa075>.
- 351 [2] M. Simonetti, N. Zhang, L. Harbers, M.G. Milia, S. Brossa, T.T. Huong Nguyen, F. Cerutti,  
352 E. Berrino, A. Sapino, M. Bienko, A. Sottile, V. Ghisetti, N. Crosetto, COVseq is a cost-  
353 effective workflow for mass-scale SARS-CoV-2 genomic surveillance, *Nat Commun.* 12  
354 (2021) 3903. <https://doi.org/10.1038/s41467-021-24078-9>.
- 355 [3] C.-C. Lo, M. Shakya, R. Connor, K. Davenport, M. Flynn, A.M. y Gutiérrez, B. Hu, P.-E.  
356 Li, E.P. Jackson, Y. Xu, P.S.G. Chain, EDGE COVID-19: a web platform to generate  
357 submission-ready genomes from SARS-CoV-2 sequencing efforts, *Bioinformatics.* (2022)  
358 btac176. <https://doi.org/10.1093/bioinformatics/btac176>.
- 359 [4] P.T. Truong Nguyen, I. Plyusnin, T. Sironen, O. Vapalahti, R. Kant, T. Smura, HAVoC, a  
360 bioinformatic pipeline for reference-based consensus assembly and lineage assignment for  
361 SARS-CoV-2 sequences, *BMC Bioinformatics.* 22 (2021) 373.  
362 <https://doi.org/10.1186/s12859-021-04294-2>.
- 363 [5] F.Z. Dezordi, A.M. da S. Neto, T. de L. Campos, P.M.C. Jeronimo, C.F. Aksenon, S.P.  
364 Almeida, G.L. Wallau, null On Behalf Of The Fiocruz Covid-Genomic Surveillance  
365 Network, ViralFlow: A Versatile Automated Workflow for SARS-CoV-2 Genome  
366 Assembly, Lineage Assignment, Mutations and Intrahost Variant Detection, *Viruses.* 14  
367 (2022) 217. <https://doi.org/10.3390/v14020217>.
- 368 [6] J. Phelan, W. Deelder, D. Ward, S. Campino, M.L. Hibberd, T.G. Clark, COVID-profiler: a  
369 webserver for the analysis of SARS-CoV-2 sequencing data, *BMC Bioinformatics.* 23  
370 (2022) 137. <https://doi.org/10.1186/s12859-022-04632-y>.
- 371 [7] W. Maier, S. Bray, M. van den Beek, D. Bouvier, N. Coraor, M. Miladi, B. Singh, J.R. De  
372 Argila, D. Baker, N. Roach, S. Gladman, F. Coppens, D.P. Martin, A. Lonie, B. Grüning,  
373 S.L. Kosakovsky Pond, A. Nekrutenko, Ready-to-use public infrastructure for global  
374 SARS-CoV-2 monitoring, *Nat Biotechnol.* (2021) 1–2. <https://doi.org/10.1038/s41587-021-01069-1>.
- 376 [8] R.R.M. Oliveira, T.C. Negri, G. Nunes, I. Medeiros, G. Araújo, F. de O. Silva, J.E.S. de  
377 Souza, R. Alves, G. Oliveira, PipeCoV: a pipeline for SARS-CoV-2 genome assembly,  
378 annotation and variant identification, *PeerJ.* 10 (2022) e13300.  
379 <https://doi.org/10.7717/peerj.13300>.
- 380 [9] P.L. Tzou, K. Tao, S.L.K. Pond, R.W. Shafer, Coronavirus Resistance Database (CoV-  
381 RDB): SARS-CoV-2 susceptibility to monoclonal antibodies, convalescent plasma, and  
382 plasma from vaccinated persons, *PLOS ONE.* 17 (2022) e0261045.  
383 <https://doi.org/10.1371/journal.pone.0261045>.
- 384 [10] R. Paredes, P.L. Tzou, G. van Zyl, G. Barrow, R. Camacho, S. Carmona, P.M. Grant, R.K.  
385 Gupta, R.L. Hamers, P.R. Harrigan, M.R. Jordan, R. Kantor, D.A. Katzenstein, D.R.  
386 Kuritzkes, F. Maldarelli, D. Otelea, C.L. Wallis, J.M. Schapiro, R.W. Shafer, Collaborative  
387 update of a rule-based expert system for HIV-1 genotypic resistance test interpretation,  
388 *PLoS ONE.* 12 (2017) e0181357. <https://doi.org/10.1371/journal.pone.0181357>.
- 389 [11] P.L. Tzou, S.L. Kosakovsky Pond, S. Avila-Rios, S.P. Holmes, R. Kantor, R.W. Shafer,  
390 Analysis of unusual and signature APOBEC-mutations in HIV-1 pol next-generation  
391 sequences, *PLoS One.* 15 (2020) e0225352. <https://doi.org/10.1371/journal.pone.0225352>.

- 392 [12] Y. Kodama, M. Shumway, R. Leinonen, International Nucleotide Sequence Database  
393 Collaboration, The Sequence Read Archive: explosive growth of sequencing data, *Nucleic*  
394 *Acids Res.* 40 (2012) D54-56. <https://doi.org/10.1093/nar/gkr854>.
- 395 [13] Y. Shu, J. McCauley, GISAID: Global initiative on sharing all influenza data – from vision  
396 to reality, *Euro Surveill.* 22 (2017) 30494. [https://doi.org/10.2807/1560-](https://doi.org/10.2807/1560-7917.ES.2017.22.13.30494)  
397 [7917.ES.2017.22.13.30494](https://doi.org/10.2807/1560-7917.ES.2017.22.13.30494).
- 398 [14] H. Li, Minimap2: pairwise alignment for nucleotide sequences, *Bioinformatics.* 34 (2018)  
399 3094–3100. <https://doi.org/10.1093/bioinformatics/bty191>.
- 400 [15] H. Li, B. Handsaker, A. Wysoker, T. Fennell, J. Ruan, N. Homer, G. Marth, G. Abecasis, R.  
401 Durbin, 1000 Genome Project Data Processing Subgroup, The Sequence Alignment/Map  
402 format and SAMtools, *Bioinformatics.* 25 (2009) 2078–2079.  
403 <https://doi.org/10.1093/bioinformatics/btp352>.
- 404 [16] M. Martin, Cutadapt removes adapter sequences from high-throughput sequencing reads,  
405 *EMBnet.Journal.* 17 (2011) 10–12. <https://doi.org/10.14806/ej.17.1.200>.
- 406 [17] N.D. Grubaugh, K. Gangavarapu, J. Quick, N.L. Matteson, J.G. De Jesus, B.J. Main, A.L.  
407 Tan, L.M. Paul, D.E. Brackney, S. Grewal, N. Gurfield, K.K.A. Van Rompay, S. Isern, S.F.  
408 Michael, L.L. Coffey, N.J. Loman, K.G. Andersen, An amplicon-based sequencing  
409 framework for accurately measuring intrahost virus diversity using PrimalSeq and iVar,  
410 *Genome Biology.* 20 (2019) 8. <https://doi.org/10.1186/s13059-018-1618-7>.
- 411 [18] Á. O'Toole, E. Scher, A. Underwood, B. Jackson, V. Hill, J.T. McCrone, R. Colquhoun, C.  
412 Ruis, K. Abu-Dahab, B. Taylor, C. Yeats, L. du Plessis, D. Maloney, N. Medd, S.W.  
413 Attwood, D.M. Aanensen, E.C. Holmes, O.G. Pybus, A. Rambaut, Assignment of  
414 epidemiological lineages in an emerging pandemic using the pangolin tool, *Virus Evolution.*  
415 7 (2021). <https://doi.org/10.1093/ve/veab064>.
- 416 [19] D.P. Martin, S. Lytras, A.G. Lucaci, W. Maier, B. Grüning, S.D. Shank, S. Weaver, O.A.  
417 MacLean, R.J. Orton, P. Lemey, M.F. Boni, H. Tegally, G.W. Harkins, C. Scheepers, J.N.  
418 Bhiman, J. Everatt, D.G. Amoako, J.E. San, J. Giandhari, A. Sigal, C. Williamson, N. Hsiao,  
419 A. von Gottberg, A. De Klerk, R.W. Shafer, D.L. Robertson, R.J. Wilkinson, B.T. Sewell,  
420 R. Lessells, A. Nekrutenko, A.J. Greaney, T.N. Starr, J.D. Bloom, B. Murrell, E. Wilkinson,  
421 R.K. Gupta, T. de Oliveira, S.L. Kosakovsky Pond, Selection Analysis Identifies Clusters  
422 of Unusual Mutational Changes in Omicron Lineage BA.1 That Likely Impact Spike  
423 Function, *Molecular Biology and Evolution.* 39 (2022) msac061.  
424 <https://doi.org/10.1093/molbev/msac061>.
- 425 [20] T.N. Starr, A.J. Greaney, S.K. Hilton, D. Ellis, K.H.D. Crawford, A.S. Dingens, M.J.  
426 Navarro, J.E. Bowen, M.A. Tortorici, A.C. Walls, N.P. King, D. Veelsler, J.D. Bloom, Deep  
427 Mutational Scanning of SARS-CoV-2 Receptor Binding Domain Reveals Constraints on  
428 Folding and ACE2 Binding, *Cell.* 182 (2020) 1295-1310.e20.  
429 <https://doi.org/10.1016/j.cell.2020.08.012>.
- 430 [21] T.N. Starr, A.J. Greaney, A. Addetia, W.W. Hannon, M.C. Choudhary, A.S. Dingens, J.Z.  
431 Li, J.D. Bloom, Prospective mapping of viral mutations that escape antibodies used to treat  
432 COVID-19, *Science.* 371 (2021) 850–854. <https://doi.org/10.1126/science.abf9302>.
- 433 [22] FDA, Fact sheet for healthcare providers: Emergency use authorization for Paxlovid, (2021).  
434 <https://www.fda.gov/media/155050/download> (accessed February 12, 2022).
- 435 [23] S. Iketani, H. Mohri, B. Culbertson, S.J. Hong, Y. Duan, M.I. Luck, M.K. Annavajhala, Y.  
436 Guo, Z. Sheng, A.-C. Uhlemann, S.P. Goff, Y. Sabo, H. Yang, A. Chavez, D.D. Ho,

- 437 Multiple pathways for SARS-CoV-2 resistance to nirmatrelvir, (2022) 2022.08.07.499047.  
438 <https://doi.org/10.1101/2022.08.07.499047>.
- 439 [24] Y. Zhou, K.A. Gammeltoft, L.A. Ryberg, L.V. Pham, U. Fahnoe, A. Binderup, C.R.D.  
440 Hernandez, A. Offersgaard, C. Fernandez-Antunez, G.H.J. Peters, S. Ramirez, J. Bukh, J.M.  
441 Gottwein, Nirmatrelvir Resistant SARS-CoV-2 Variants with High Fitness in Vitro, (2022)  
442 2022.06.06.494921. <https://doi.org/10.1101/2022.06.06.494921>.
- 443 [25] D. Jochmans, C. Liu, K. Donckers, A. Stoycheva, S. Boland, S.K. Stevens, C.D. Vita, B.  
444 Vanmechelen, P. Maes, B.S. Trüeb, N. Ebert, V. Thiel, S.D. Jonghe, L. Vangeel, D. Bardiot,  
445 A. Jekle, L.M. Blatt, L. Beigelman, J.A. Symons, P. Raboisson, P. Chaltin, A. Marchand, J.  
446 Neyts, J. Deval, K. Vanduyck, The substitutions L50F, E166A and L167F in SARS-CoV-2  
447 3CLpro are selected by a protease inhibitor in vitro and confer resistance to nirmatrelvir,  
448 (2022) 2022.06.07.495116. <https://doi.org/10.1101/2022.06.07.495116>.
- 449 [26] E. Heilmann, F. Costacurta, A. Volland, D. von Laer, SARS-CoV-2 3CLpro mutations  
450 confer resistance to Paxlovid (nirmatrelvir/ritonavir) in a VSV-based, non-gain-of-function  
451 system, (2022) 2022.07.02.495455. <https://doi.org/10.1101/2022.07.02.495455>.
- 452 [27] S. Iketani, S.J. Hong, J. Sheng, F. Bahari, B. Culbertson, F.F. Atanaki, A.K. Aditham, A.F.  
453 Kratz, M.I. Luck, R. Tian, S.P. Goff, H. Montazeri, Y. Sabo, D.D. Ho, A. Chavez,  
454 Functional map of SARS-CoV-2 3CL protease reveals tolerant and immutable sites, *Cell*  
455 *Host & Microbe*. (2022). <https://doi.org/10.1016/j.chom.2022.08.003>.
- 456 [28] G.D. Noske, E. de S. Silva, M.O. de Godoy, I. Dolci, R.S. Fernandes, R.V.C. Guido, P. Sjö,  
457 G. Oliva, A.S. Godoy, Structural basis of nirmatrelvir and ensitrelvir resistance profiles  
458 against SARS-CoV-2 Main Protease naturally occurring polymorphisms, (2022)  
459 2022.08.31.506107. <https://doi.org/10.1101/2022.08.31.506107>.
- 460 [29] Y. Hu, E.M. Lewandowski, H. Tan, R.T. Morgan, X. Zhang, L.M.C. Jacobs, S.G. Butler,  
461 M.V. Mongora, J. Choy, Y. Chen, J. Wang, Naturally occurring mutations of SARS-CoV-2  
462 main protease confer drug resistance to nirmatrelvir, (2022) 2022.06.28.497978.  
463 <https://doi.org/10.1101/2022.06.28.497978>.
- 464 [30] V.M. de Oliveira, M.F. Ibrahim, X. Sun, R. Hilgenfeld, J. Shen, H172Y mutation perturbs  
465 the S1 pocket and nirmatrelvir binding of SARS-CoV-2 main protease through a nonnative  
466 hydrogen bond, (2022) 2022.07.31.502215. <https://doi.org/10.1101/2022.07.31.502215>.
- 467 [31] V.M. Sasi, S. Ullrich, J. Ton, S.E. Fry, J. Johansen-Leete, R.J. Payne, C. Nitsche, C.J.  
468 Jackson, Predicting antiviral resistance mutations in SARS-CoV-2 main protease with  
469 computational and experimental screening, (2022) 2022.08.24.505060.  
470 <https://doi.org/10.1101/2022.08.24.505060>.
- 471 [32] S.A. Moghadasi, E. Heilmann, S.N. Moraes, F.L. Kearns, D. von Laer, R.E. Amaro, R.S.  
472 Harris, Transmissible SARS-CoV-2 variants with resistance to clinical protease inhibitors,  
473 (2022) 2022.08.07.503099. <https://doi.org/10.1101/2022.08.07.503099>.
- 474 [33] J. Ou, E.M. Lewandowski, Y. Hu, A.A. Lipinski, R.T. Morgan, L.M.C. Jacobs, X. Zhang,  
475 M.J. Bikowitz, P. Langlais, H. Tan, J. Wang, Y. Chen, J.S. Choy, A yeast-based system to  
476 study SARS-CoV-2 Mpro structure and to identify nirmatrelvir resistant mutations, (2022)  
477 2022.08.06.503039. <https://doi.org/10.1101/2022.08.06.503039>.
- 478 [34] A.M. Shaqra, S.N. Zvornicanin, Q.Y.J. Huang, G.J. Lockbaum, M. Knapp, L. Tandeske,  
479 D.T. Bakan, J. Flynn, D.N.A. Bolon, S. Moquin, D. Dovala, N. Kurt Yilmaz, C.A. Schiffer,  
480 Defining the substrate envelope of SARS-CoV-2 main protease to predict and avoid drug  
481 resistance, *Nat Commun.* 13 (2022) 3556. <https://doi.org/10.1038/s41467-022-31210-w>.



- 482 [35] K.S. Yang, S.Z. Leeuwon, S. Xu, W.R. Liu, Evolutionary and Structural Insights about  
483 Potential SARS-CoV-2 Evasion of Nirmatrelvir, *J. Med. Chem.* 65 (2022) 8686–8698.  
484 <https://doi.org/10.1021/acs.jmedchem.2c00404>.
- 485 [36] S. Gandhi, J. Klein, A.J. Robertson, M.A. Peña-Hernández, M.J. Lin, P. Roychoudhury, P.  
486 Lu, J. Fournier, D. Ferguson, S.A.K. Mohamed Bakhsh, M. Catherine Muenker, A.  
487 Srivathsan, E.A. Wunder, N. Kerantzas, W. Wang, B. Lindenbach, A. Pyle, C.B. Wilen, O.  
488 Ogbuagu, A.L. Greninger, A. Iwasaki, W.L. Schulz, A.I. Ko, De novo emergence of a  
489 remdesivir resistance mutation during treatment of persistent SARS-CoV-2 infection in an  
490 immunocompromised patient: a case report, *Nat Commun.* 13 (2022) 1547.  
491 <https://doi.org/10.1038/s41467-022-29104-y>.
- 492 [37] J.I. Hogan, R. Duerr, D. Dimartino, C. Marier, S.E. Hochman, S. Mehta, G. Wang, A.  
493 Heguy, Remdesivir resistance in transplant recipients with persistent COVID-19, *Clinical*  
494 *Infectious Diseases.* (2022) ciac769. <https://doi.org/10.1093/cid/ciac769>.
- 495 [38] M. Martinot, A. Jary, S. Fafi-Kremer, V. Leducq, H. Delagreverie, M. Garnier, J.  
496 Pacanowski, A. Mékinian, F. Pirenne, P. Tiberghien, V. Calvez, C. Humbrecht, A.-G.  
497 Marcelin, K. Lacombe, Emerging RNA-Dependent RNA Polymerase Mutation in a  
498 Remdesivir-Treated B-cell Immunodeficient Patient With Protracted Coronavirus Disease  
499 2019, *Clin Infect Dis.* 73 (2021) e1762–e1765. <https://doi.org/10.1093/cid/ciaa1474>.
- 500 [39] A. Heyer, T. Günther, A. Robitaille, M. Lütgehetmann, M.M. Addo, D. Jarczак, S. Kluge,  
501 M. Aepfelbacher, J. Schulze zur Wiesch, N. Fischer, A. Grundhoff, Remdesivir-induced  
502 emergence of SARS-CoV2 variants in patients with prolonged infection, *Cell Reports*  
503 *Medicine.* 3 (2022) 100735. <https://doi.org/10.1016/j.xcrm.2022.100735>.
- 504 [40] L.J. Stevens, A.J. Pruijssers, H.W. Lee, C.J. Gordon, E.P. Tchesnokov, J. Gribble, A.S.  
505 George, T.M. Hughes, X. Lu, J. Li, J.K. Perry, D.P. Porter, T. Cihlar, T.P. Sheahan, R.S.  
506 Baric, M. Götte, M.R. Denison, Distinct genetic determinants and mechanisms of SARS-  
507 CoV-2 resistance to remdesivir, (2022) 2022.01.25.477724.  
508 <https://doi.org/10.1101/2022.01.25.477724>.
- 509 [41] L. Checkmahomed, J. Carbonneau, V. Du Pont, N.C. Riola, J.K. Perry, J. Li, B. Paré, S.M.  
510 Simpson, M.A. Smith, D.P. Porter, G. Boivin, In Vitro Selection of Remdesivir-Resistant  
511 SARS-CoV-2 Demonstrates High Barrier to Resistance, *Antimicrobial Agents and*  
512 *Chemotherapy.* 0 (n.d.) e00198-22. <https://doi.org/10.1128/aac.00198-22>.
- 513 [42] A.M. Szemiel, A. Merits, R.J. Orton, O.A. MacLean, R.M. Pinto, A. Wickenhagen, G.  
514 Lieber, M.L. Turnbull, S. Wang, W. Furnon, N.M. Suarez, D. Mair, A. da S. Filipe, B.J.  
515 Willett, S.J. Wilson, A.H. Patel, E.C. Thomson, M. Palmarini, A. Kohl, M.E. Stewart, In  
516 vitro selection of Remdesivir resistance suggests evolutionary predictability of SARS-CoV-  
517 2, *PLOS Pathogens.* 17 (2021) e1009929. <https://doi.org/10.1371/journal.ppat.1009929>.
- 518 [43] M.L. Agostini, E.L. Andres, A.C. Sims, R.L. Graham, T.P. Sheahan, X. Lu, E.C. Smith, J.B.  
519 Case, J.Y. Feng, R. Jordan, A.S. Ray, T. Cihlar, D. Siegel, R.L. Mackman, M.O. Clarke,  
520 R.S. Baric, M.R. Denison, Coronavirus Susceptibility to the Antiviral Remdesivir (GS-5734)  
521 Is Mediated by the Viral Polymerase and the Proofreading Exoribonuclease, *MBio.* 9 (2018)  
522 e00221-18. <https://doi.org/10.1128/mBio.00221-18>.
- 523 [44] P.S.-W. Yeung, H. Wang, M. Sibai, D. Solis, F. Yamamoto, N. Iwai, B. Jiang, N.  
524 Hammond, B. Truong, S. Bihon, S. Santos, M. Mar, C. Mai, K.O. Mfuh, J.A. Miller, C.  
525 Huang, M.K. Sahoo, J.L. Zehnder, B.A. Pinsky, Evaluation of a Rapid and Accessible  
526 Reverse Transcription-Quantitative PCR Approach for SARS-CoV-2 Variant of Concern  
527 Identification, *J Clin Microbiol.* 60 (n.d.) e00178-22. <https://doi.org/10.1128/jcm.00178-22>.

- 528 [45] S. Khare, C. Gurry, L. Freitas, M.B. Schultz, G. Bach, A. Diallo, N. Akite, J. Ho, R.T. Lee,  
529 W. Yeo, G.C. Curation Team, S. Maurer-Stroh, GISAID's Role in Pandemic Response,  
530 China CDC Wkly. 3 (2021) 1049–1051. <https://doi.org/10.46234/ccdcw2021.255>.
- 531 [46] S.L.K. Pond, SARS-CoV-2-variation/variation-new at master · spond/SARS-CoV-2-  
532 variation, GitHub. (2022). <https://github.com/spond/SARS-CoV-2-variation> (accessed  
533 October 3, 2022).
- 534 [47] D.P. Martin, S. Weaver, H. Tegally, J.E. San, S.D. Shank, E. Wilkinson, A.G. Lucaci, J.  
535 Giandhari, S. Naidoo, Y. Pillay, L. Singh, R.J. Lessells, R.K. Gupta, J.O. Wertheim, A.  
536 Nekturenko, B. Murrell, G.W. Harkins, P. Lemey, O.A. MacLean, D.L. Robertson, T. de  
537 Oliveira, S.L. Kosakovsky Pond, The emergence and ongoing convergent evolution of the  
538 SARS-CoV-2 N501Y lineages, *Cell*. 184 (2021) 5189–5200.e7.  
539 <https://doi.org/10.1016/j.cell.2021.09.003>.
- 540 [48] E.B. Hodcroft, CoVariants: SARS-CoV-2 Mutations and Variants of Interest., (2021).  
541 <https://covariants.org/> (accessed May 29, 2022).
- 542 [49] M. McCallum, N. Czudnochowski, L.E. Rosen, S.K. Zepeda, J.E. Bowen, A.C. Walls, K.  
543 Hauser, A. Joshi, C. Stewart, J.R. Dillen, A.E. Powell, T.I. Croll, J. Nix, H.W. Virgin, D.  
544 Corti, G. Snell, D. Veessler, Structural basis of SARS-CoV-2 Omicron immune evasion and  
545 receptor engagement, *Science*. (2022) eabn8652. <https://doi.org/10.1126/science.abn8652>.
- 546 [50] K. Gangavarapu, A.A. Latiff, J.L. Mullen, M. Alkuzweny, E. Hufbauer, G. Tsueng, E.  
547 Haag, M. Zeller, C.M. Aceves, K. Zaiets, M. Cano, J. Zhou, Z. Qian, R. Sattler, N.L.  
548 Matteson, J.I. Levy, M.A. Suchard, C. Wu, A.I. Su, K.G. Andersen, L.D. Hughes,  
549 Outbreak.info genomic reports: scalable and dynamic surveillance of SARS-CoV-2 variants  
550 and mutations, (2022) 2022.01.27.22269965. <https://doi.org/10.1101/2022.01.27.22269965>.
- 551 [51] W. Yin, Y. Xu, P. Xu, X. Cao, C. Wu, C. Gu, X. He, X. Wang, S. Huang, Q. Yuan, K. Wu,  
552 W. Hu, Z. Huang, J. Liu, Z. Wang, F. Jia, K. Xia, P. Liu, X. Wang, B. Song, J. Zheng, H.  
553 Jiang, X. Cheng, Y. Jiang, S.-J. Deng, H.E. Xu, Structures of the Omicron spike trimer with  
554 ACE2 and an anti-Omicron antibody, *Science*. 375 (2022) 1048–1053.  
555 <https://doi.org/10.1126/science.abn8863>.
- 556 [52] N. Ikemura, S. Taminishi, T. Inaba, T. Arimori, D. Motooka, K. Katoh, Y. Kirita, Y.  
557 Higuchi, S. Li, T. Suzuki, Y. Itoh, Y. Ozaki, S. Nakamura, S. Matoba, D.M. Standley, T.  
558 Okamoto, J. Takagi, A. Hoshino, An engineered ACE2 decoy neutralizes the SARS-CoV-2  
559 Omicron variant and confers protection against infection in vivo, *Science Translational*  
560 *Medicine*. 0 (2022) eabn7737. <https://doi.org/10.1126/scitranslmed.abn7737>.
- 561 [53] Y. Cao, F. Jian, J. Wang, Y. Yu, W. Song, A. Yisimayi, J. Wang, R. An, N. Zhang, Y.  
562 Wang, P. Wang, L. Zhao, H. Sun, L. Yu, S. Yang, X. Niu, T. Xiao, Q. Gu, F. Shao, X. Hao,  
563 Y. Xu, R. Jin, Y. Wang, X.S. Xie, Imprinted SARS-CoV-2 humoral immunity induces  
564 convergent Omicron RBD evolution, (2022) 2022.09.15.507787.  
565 <https://doi.org/10.1101/2022.09.15.507787>.
- 566
- 567
- 568
- 569
- 570

571 **Declaration of interests**

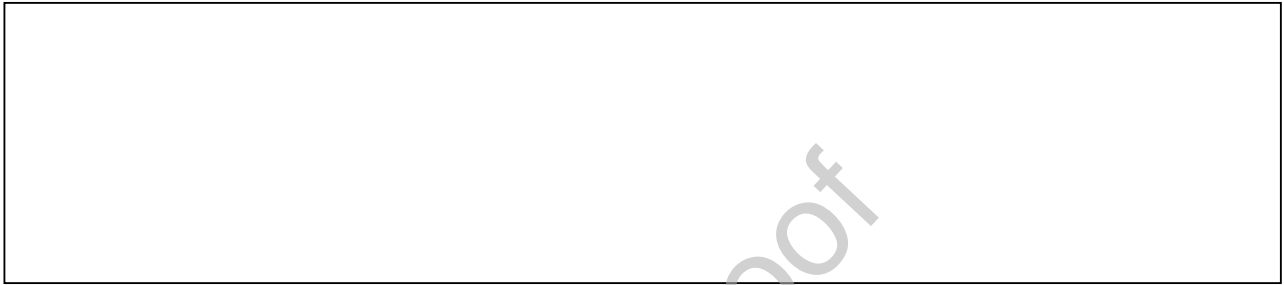
572

573  The authors declare that they have no known competing financial interests or personal  
574 relationships that could have appeared to influence the work reported in this paper.

575

576  The authors declare the following financial interests/personal relationships which may be considered  
577 as potential competing interests:

578



579

580

581

582

583

Journal Pre-proof